BMC Plant Biology

RESEARCH Open Access

Graphene nanomaterials and copper co-exposure in *Populus nigra* L.: ultrastructural, biochemical, and nutritional impact under *in vitro* conditions

Simonetta Muccifora[1], Maria Adelaide Iannelli[2], Barbara Casentini[3], Lorenzo Camoni[4], Anna Fiorillo[4], Davide Gentile[2], Manuela Melucci[5], Valerio Giorgio Muzzini[6] and Valentina Iori[2*]

Abstract

The wide application of graphene nanomaterials has led to their release into the environment, raising ecological risk concerns, especially when co-existing with other pollutants like copper (Cu), one of the most ubiquitous environmental metals. The impact of co-presence of these nanomaterials and Cu on woody plants remains unstudied and, in this regard, callus culture represents a reliable tool for toxicological studies. In this work, we investigated the effects of Cu in combination with two different graphene nanomaterials, graphene oxide (GO) and graphene nanoplatelets (GNP), on the cell ultrastructure, biochemical responses and nutrient uptake in callus culture of *Populus nigra* L., a pioneer tree species in the riparian ecosystem. GO and GNP alone showed an adverse impact on poplar cells, causing a significant reduction in dry weight and a notable increase in MDA levels, water and Ca uptake, and protein synthesis. Co-exposure to Cu and either GO or GNP increased dry weight while decreasing water content, MDA levels, antioxidant enzyme activities, and protein content. Furthermore, GO + Cu exposure promoted greater cellular metal uptake than the GNP + Cu treatment, indicating a greater effectiveness of GO as a Cu carrier, due to the higher presence of oxygen functional groups on its surface than GNP. Transmission Electron Microscopy (TEM) observations confirmed the cellular uptake of both GO and GNP, revealing distinct impacts on cell ultrastructure. These results provide useful information on the interaction between graphene nanomaterials and Cu for risk assessment and developing sustainable management strategies in agro-forestry.

Keywords Poplar, Oxidative stress, Heavy metal, Cell ultrastructure, H^+-ATPase activity, Phytotoxicity

*Correspondence:
Valentina Iori
valentina.iori@cnr.it
[1]Department of Life Sciences, University of Siena, Via A. Moro 2, Siena 53100, Italy
[2]Institute of Agricultural Biology and Biotechnology - National Research Council (CNR-IBBA), Section of Rome, Strada provinciale 35d, 9, Montelibretti, Rome 00010, Italy
[3]Water Research Institute - National Research Council (CNR-IRSA), Strada provinciale 35d, 9, Montelibretti, Rome 00010, Italy
[4]Department of Biology, Tor Vergata University of Rome, Via della Ricerca Scientifica, Rome 00133, Italy
[5]Institute for Organic Synthesis and Photoreactivity - National Research Council (CNR-ISOF), via Piero Gobetti 101, Bologna 40129, Italy
[6]Institute for Biological Systems - National Research Council (CNR-ISB), Strada provinciale 35d, 9, Montelibretti, Rome 00010, Italy

Introduction

Due to their unique properties and low production costs, there is a growing interest in graphene nanomaterials, leading to their widespread application in industrial and agricultural sectors. Graphene nanomaterials include several forms, such as graphene-oxide (GO) and graphene nanoplatelets (GNP), characterized by differences in their surface chemistry, layer number, lateral size, and degree of oxidation [1]. GO - the oxidized form of graphene - has garnered widespread application in various fields, including biomedicine, electronics, packaging, biosensors, semiconductors, wastewater and drinking water treatment [2, 3]. GO's surface is rich in oxygen-containing functional groups (epoxy, hydroxyl, carboxyl, and carbonyl), which play a key role in determining its solubility and molecular adsorption properties [4]. To date, most research focuses on GO's high adsorption efficiency for environmental decontamination. For instance, GO was successfully used for the removal of heavy metal ions, pharmaceuticals and persistent organic pollutants from water [5, 6]. In recent years, GO has triggered enormous interest in applications in agro-forestry to boost plant growth and stress tolerance. Due to the presence of a large surface area and a high density of surface oxygen binding sites, GO has been extensively used in efforts to develop a new generation of slow- or controlled-release fertilizers [7]. For instance, the efficacy of GO-based carriers was demonstrated for the delivery of Zn and Cu with a promising performance compared to commercial soluble fertilizers [4]. Instead, GNP is widely used in industrial applications primarily due to its superior mechanical, thermal, and electrical properties. Recently, this nanomaterial has gained significant attention for the development of sustainable graphene-based composites with high adsorption capacity for water purification [8–10].

The widespread and excessive application of these nanomaterials has inevitably led to their release into the environment at all stages of their lifecycle, raising serious concerns regarding both ecological safety and potential human health implications [11]. Overall, the actual environmental discharge of graphene-related materials following their end-of-life remains unquantified [12]. Recently, based on predictive models, by 2030 the concentrations of graphene nanomaterials will be 1.4 ng/L in surface water, 16 ng/kg in natural/urban soil, and 20 µg/kg in sludge-treated soil [13].

To date, most scientific literature has focused on the impact of GO on plants, reporting conflicting findings, ranging from stimulation and inhibition to no observable effects on plant growth and development. Such variability is contingent upon the concentration and timing of exposure, experimental settings, and the specific plant species under study [1, 14]. For instance, exposure to low concentrations of GO (50 and 100 mg/L) was found to promote tomato plant growth by stimulating cell division in the shoot [15]. Similar growth-promoting effects were observed in *Aloe vera* L. at 10-100 mg/L due to enhanced photosynthesis [16] while 20 mg/L of GO increased the number of adventitious roots in tobacco seedlings [17]. Conversely, a 15-day treatment with 50 mg/L GO reduced root length as well as fresh and dry weight in five different rice species [18]; similarly, the fresh root weight of *Brassica napus* L. decreased when exposed to GO concentrations of 50-100 mg/L [19]. However, studies on GNP are very limited. For instance, GNP treatment (1000 mg/L) under water deficit stress significantly improved fruit production and fruit dry weight in bell pepper plants [20].

Nonetheless, these investigations primarily focus on the phytotoxic effects of GO and GNP alone, without accounting for their potential interactions and co-existence with other substances following environmental release. In nature, chemical pollutants are typically found as complex mixtures where they can interact with each other. The combined impact of these contaminants can differ from their individual effects, resulting in synergistic (enhanced) or antagonistic (reduced) interactions [21]. Heavy metals are among the most widespread and well-known environmental pollutants, with serious implications for human health. Therefore, the likelihood of GO and GNP interacting with metal ions in natural ecosystems is a critical factor, as such interactions can alter the bioavailability and toxicity of both the metals and the nanomaterials.

Copper (Cu) is an essential micronutrient for proper plant growth and development, yet it is also one of the most ubiquitous and environmentally impactful heavy metals. The extensive application of agrochemicals, like fertilizers and pesticides, has significantly raised environmental Cu levels, thereby compromising long-term agricultural productivity [22]. This element exhibits a dual function in plant metabolism, contingent upon its concentration in tissues. At low levels, Cu is involved in several physiological and biochemical processes such as photosynthesis, protein transport, carbohydrate and cell wall metabolism, and hormone signal transduction. Acting as a co-factor for a range of oxygen-processing enzymes, including polyphenol oxidase, Cu/Zn-superoxide dismutase, amino oxidase, ascorbate oxidase, and plastocyanin, Cu significantly contributes to oxidative stress mitigation, thereby enhancing the plant's ability to withstand various abiotic stresses [23]. On the other hand, high levels of Cu have a detrimental effect, interfering with plant growth and metabolism and altering the function of proteins, lipids, DNA and RNA [24].

Currently, studies on the effects of GO and GNP on the biological Cu behaviour in plants are still scarce and

inconsistent. For example, GO exposure mitigated the damage caused by Cu stress (5-20 µM) in *Lemna minor* [2] whereas, the addition of carboxylate GO-chitosan spheres reduced Cu bioaccumulation by about 50% in wheat seedlings grown in soil contaminated with 120 mg/L Cu [25]. Analogously, co-exposure to 1 mg/L Cd and 10 mg/L GO nanosheets was found to alleviate the adverse effects of the metal while simultaneously enhancing Cd accumulation in hydroponically grown rice seedlings [26]. Furthermore, the co-exposure of soybean seedlings to cerium oxide nanoparticles (CeO_2NPs) and Cd led to higher excretion of plant root exudates, which modified rhizosphere chemistry and promoted CeO_2NPs dissolution, thereby increasing Ce accumulation in the shoots. Conversely, CeO_2NPs provided adsorption sites for Cd, reducing its uptake into the plants [27].

To date, there is a significant knowledge gap regarding the interactive effects of co-exposure to Cu and either GO or GNP on woody plants. In this regard, black poplar (*Populus nigra* L.) is considered a model species in abiotic stress studies, whose ability to tolerate environmental pollutants has been previously explored in in vitro approaches [28, 29]. The use of in vitro assays is a well-established tool for assessing stress responses in plants, particularly in woody species exhibiting long reproductive cycles [30]. Hence, the present study investigated the effects of Cu in the co-presence of GO or GNP on *P. nigra* (clone 58–861) callus cultures. Specifically, we examined poplar cell ultrastructure, antioxidant enzyme activities, Cu uptake and the underlying mechanisms of the observed changes. We assumed that when combined, GO + Cu or GNP + Cu would induce a biochemical response that is significantly different from the effects observed with the individual application of Cu, GO, or GNP. The results could provide useful information on the impact of graphene nanomaterials and Cu for risk assessment and developing sustainable management strategies in agro-forestry.

Table 1 The XPS atomic composition, the O/C ratio and the origin of GO and GNP. The bibliographic reference providing the detailed material characterization is listed for each material

Material	Origin	XPS atomic composition	O/C ratio	References
GO	LayerOne	C 70.1%, O 27.2%, N 0.2%, S 1.0%, Si 0.8%, Cl 0.7%, Mn below 0.1%	0.39	[8]
GNP	Euronova Next-Generation Sustainable Plastic Materials Company	C 87%, O 9%, Fe 0.5%, other elements 3.5%	0.05	[10, 31]

Materials and methods

Graphene nanomaterials

GO was purchased from LayerOne, while GNP was produced from waste tires by the patented technology (B. Saner Okan, *A Sustainable and Scalable Method For Graphene Production*, PCT Application, PCT/TR2024/050394, 2024) and provided by Euronova Next-Generation Sustainable Plastic Materials Company (Türkiye). Both nanomaterials were rinsed with ultrapure water to remove any potential mobile metal residues. The adsorption kinetics of Cu on both GO and GNP in Milli-Q solution are presented in Supplementary Fig. S1.

The XPS atomic composition and the O/C ratio of the two materials are reported in Table 1. The detailed characterization of their structural and morphological properties is available in the cited references.

Plant material and experimental setup

Plant material was obtained from the experimental field at the Regional Research Campus of Rome 1 in Montelibretti (ARRM1) (formerly managed by CNR-IBAF) and has been maintained by the CNR-IBBA according to the protocol described in Iori et al. [28]. Poplar calli were grown in Petri dishes on Murashige and Skoog (MS) nutrient medium [32] containing sucrose (30 g/L), kinetin (0.7 mg/L), and 2,4-dichlorophenoxyacetic acid (2,4-D) (1 mg/L). The medium was solidified with agar (7 g/L) and adjusted to pH 5.7. For the combined treatments, a concentration of 3.18 mg/L Cu (corresponding to a sub-lethal EC_{20} value of 50 µM) was applied based on preliminary dose-response assays, which established the Cu tolerance range for clone 58–861. A concentration of 25 mg/L for both GO and GNP was selected based on its ability to induce mild stress without exceeding the cytotoxicity threshold [33]. GO and GNP stock solutions were sonicated for 2 h and added to the MS medium before autoclaving, whereas the Cu stock solution was filtered and supplemented to the growth medium after sterilization. Experiments were conducted with Cu alone, and in combination with either GO or GNP. Five Petri dishes, each containing four calli, were used for every treatment and the untreated control. Cell cultures were grown at 25 °C in darkness for three weeks. After incubation, calli were collected to measure their fresh weight (FW) and total water content. Each callus was rinsed with sterilized distilled water and dried on filter paper prior to weighing. Calli were dried in an oven at 60 °C until constant weight was achieved, yielding the dry weight (DW). Water content was calculated using the formula: (FW-DW)/FW. For biochemical analysis, each callus was snap-frozen in liquid N_2 and stored at -80 °C.

Transmission electron microscopy (TEM)

GO and GNP were characterized by TEM placing a drop of the GO and GNP stock solution (1.5 g/L), diluted 1:2 with Milli-Q water, on grids covered by formvar, allowed to settle, dried, and observed under a FEI Tecnai TEM at 100 kV.

For TEM observations, at least ten callus fragments were sampled from three biological replicates per treatment. Samples were fixed in Karnovsky solution, post-fixed in osmium tetroxide, dehydrated and embedded in Epon 812-Araldite A/M mixture. Thin sections were stained with uranyl acetate and lead citrate and observed under a FEI Tecnai TEM at 100 kV.

Determination of malondialdehyde (MDA) content and antioxidant enzymatic activities

Lipid peroxidation was quantified by measuring thiobarbituric acid-reactive substances (TBARS), primarily malondialdehyde (MDA), following the protocol described by Iori et al. [29]. Briefly, frozen calli were homogenized in 0.1% TCA, and centrifuged for 15 min at 16,000 g. The supernatant was incubated with 0.5% TBA in 20% TCA and 1 mM EDTA at 95 °C for 30 min. Following centrifugation (16,000 g, 10 min), the supernatant absorbance was measured at 532 and 600 nm. MDA levels were calculated using $\varepsilon = 155\ mM\ cm^{-1}$.

Extraction and activity assays for ascorbate peroxidase (APX, EC 1.11.1.11) and catalase (CAT, EC 1.11.1.6) were performed as reported by Iori et al. [29]. Frozen calli were homogenized with ice-cold 50 mM potassium phosphate buffer (pH 7.0) containing 0.1% (w/v) ascorbic acid, 1% (w/v) polyvinylpolypyrrolidone (PVPP), 1 mM Na_2-EDTA and 0.1% (v/v) Triton X-100. The homogenate was centrifuged at 4 °C for 30 min at 15,000 g and the supernatant fraction was set aside for activity assay. APX and CAT activities were determined spectrophotometrically in 1 mL reaction mixtures (50 mM potassium phosphate buffer, pH 7.0) containing enzyme extract. APX activity was measured by monitoring ascorbate oxidation at 290 nm ($\varepsilon = 28\ mM^{-1}\ cm^{-1}$) for 1 min in the presence of 0.5 mM ascorbic acid and 10 mM H_2O_2. APX activity was expressed as µmol of ascorbate oxidized per mg^{-1} protein min^{-1}. CAT activity was determined by following H_2O_2 consumption at 240 nm ($\varepsilon = 36\ mM^{-1}\ cm^{-1}$) for 40 s with 125 mM H_2O_2. CAT activity was expressed as µmol of H_2O_2 per mg^{-1} protein min^{-1}.

All procedures followed glutathione S-transferase (GST, EC 2.5.1.18) activity was determined according to Habig and Jakoby [34], using a reaction buffer containing 0.1 M phosphate buffer (pH 6.5), 1 mM reduced glutathione (GSH), 1 mM 1-chloro-2,4-dinitrobenzene (CDNB), and the enzyme extract. The conjugation of CDNB with GSH was monitored at 340 nm ($\varepsilon = 0.0096\ \mu M^{-1}\ cm^{-1}$) at 25 °C. GST activity was expressed as mM CDNB per mg protein^{-1} min^{-1}. All spectrophotometric measurements were carried out using a Thermo Multiskan FC Microplate Photometer (Thermo Fisher Scientific, Waltham, MA, USA).

Total soluble protein content was determined according to Ernst and Zor [35], using bovine serum albumin (BSA) as a standard.

Purification of plasma membranes

Plasma membranes (PM) were purified by two-phase partitioning, as described by Fiorillo et al. [36]. Briefly, each single cultured poplar callus was weighed and homogenized with an adequate amount of a buffer (weight/volume ratio 1:1) containing 25 mM MOPS-BTP, 250 mM sucrose, 2 mM DTT, 5 mM EDTA, 1 mM PMSF, 0.2% BSA, pH 7.8, filtered with a fine weave gauze and centrifuged for 20 min at 8,000 g at 4 °C. The supernatant was ultracentrifuged at 70,000 g for 30 min, and the pelleted microsomal fraction was resuspended in 0.2 mL of 5 mM potassium phosphate buffer containing 0.2 mM PMSF, pH 7.8, and added to 1.4 mL of 5 mM potassium phosphate buffer containing 7.2% Dextran T-500, 7.2% PEG-3350, 286 mM sucrose, 5.7 mM KCl, pH 7.8. The samples were then gently mixed through repeated inversions and centrifuged at 2,000 g for 15 min at 4 °C. The plasma membranes were recovered by diluting twofold the upper phase in 10 mM MOPS-BTP, 250 mM sucrose, 2 mM EDTA, 1 mM DTT, 1 mM PMSF, pH 7.0, and centrifuging for 45 min at 125,000 g at 4 °C. Finally, the pellet was resuspended in 0.2 mL of 10 mM Tris-HCl, 1 mM EDTA, 1 mM DTT, 20% glycerol, pH 7.6.

H^+-ATPase activity

The phosphohydrolytic activity of plasma membrane samples from cultured poplar calli was assayed according to Visconti et al. [37], with minor modifications. After incubating 30 µg of two-phase partitioned PM vesicles for 30 min in 500 µL of reaction buffer (50 mM Tris-MES, 5 mM KNO_3, 5 mM $MgSO_4$, 0.2 mM $(NH_4)6Mo_7O_{24}$, 2 mM ATP, pH 6.5), the reaction was stopped with 1 mL of phosphate reagent (0.5% SDS, 0.5% $(NH_4)6Mo_7O_{24}$, 2% (v/v) H_2SO_4, 0.01% ascorbate). The phosphomolybdic acid produced was calculated by measuring the absorbance at 740 nm. The phosphate concentration was then calculated by interpolating with a calibration curve obtained with various concentrations of KH_2PO_4. For each sample, the residual activity in the presence of 0.2 mM of the H^+-ATPase inhibitor Na_3VO_4 was subtracted from the obtained values to calculate the H^+-ATPase-specific activity.

Western blot

Immunoblotting analysis was performed according to Fiorillo et al. [38], using polyclonal anti-H^+-ATPase

antibodies [39], directed against a conserved region in the C-terminal domain at 1:1000 dilution. Protein detections were performed by incubating the membrane with horseradish peroxidase-conjugated anti-rabbit secondary antibody (1:5000) from Bio-Rad.

Analysis of Cu and nutrient contents

The oven-dried calli were mineralised according to the method described by Iori et al. [29]. The concentrations of Cu and nutrients were measured by Inductively Coupled Plasma Optical Emission Spectrometry (ICP-OES, 5800 Agilent Technologies, USA-LOD = 0.02 mg/L).

Statistical analysis

The obtained data were described as the mean of three biological replicates ± standard deviations (SD). All results were checked for normality before analyses of variance by Shapiro-Wilk's test. Statistical significance was assessed using one-way analysis of variance (ANOVA) and Tukey's post hoc test, performed within the R software environment. All statistical tests were considered significant at $p < 0.05$.

Principal Component Analysis (PCA) was performed in R (version 4.5.1) to explore patterns and relationships within the multivariate dataset of biological responses to various treatments. The dataset comprised quantitative measurements of physiological (FW, DW, Water content, Protein content) and biochemical parameters (Cu content, Ca, APX, CAT, MDA, GST, ATPase activity) across six treatment groups (Control, Cu, GNP, GNP + Cu, GO, GO + Cu).

PCA was then executed using the PCA() function from the "FactoMineR" package. The data was automatically scaled to unit variance (default scale.unit = TRUE) to prevent variables with larger magnitudes from disproportionately influencing the results. Visualization of the PCA outputs was performed using the "factoextra" package. Individual plots (fviz_pca_ind) displayed samples colored by treatment group, with 95% confidence ellipses. Variable plots (fviz_pca_var) showed the contribution of each parameter to the principal components.

Table 2 Effects of GO, GNP and Cu, either alone or in combination, on Fresh weight, Dry weight and Water content in clone 58–861 (± SD, $n = 20$)

Treatments	Fresh weight (g)	Dry weight (g)	Water content (%)
Control	0.331 ± 0.057^{cd}	0.0241 ± 0.0042^{b}	92.79^{c}
GNP	0.403 ± 0.087^{b}	0.0155 ± 0.0033^{c}	96.12^{ab}
GNP + Cu	0.293 ± 0.092^{cd}	0.0405 ± 0.0128^{a}	86.19^{d}
GO	0.272 ± 0.025^{cd}	0.0051 ± 0.0006^{d}	98.01^{a}
GO + Cu	0.685 ± 0.129^{a}	0.0413 ± 0.0077^{a}	90.61^{c}
Cu	0.246 ± 0.046^{d}	0.0230 ± 0.0043^{b}	94.01^{cd}

Different letters indicate significant differences ($p \leq 0.05$, Tukey's test)

Results

Biomass production

As reported in Table 2, poplar cells exposed to GNP alone showed an increase in FW production by 22.12% compared to the control, whereas no significant difference was observed between the control and GO-treated callus cultures. Following GO + Cu treatment, a twofold enhancement of fresh weight was detected in poplar cells compared to both the control and GO-treated calli. In contrast, the co-exposure to GNP and Cu caused a decrease in FW by approximately 27% compared to GNP alone, resulting in values similar to the control. About DW, both in the presence of GNP and GO, poplar cells showed a reduction in dry weight compared to the control, being more pronounced in the GO condition (by 78.8%) than in the GNP condition (by 35.8%). Conversely, following both GO + Cu and GNP + Cu treatment, an increase of approximately 70% in DW was observed compared with the control. No difference between control and Cu-treated cells was detected in clone 58–861. As reported, the moisture content varied from 86% to 98% in all the applied treatments, resulting higher in poplar cells exposed to GO and GNP alone and lower under GNP + Cu treatment.

Due to the high water content detected within the cells of clone 58–861, all physiological parameters were calculated in relation to DW rather than FW.

TEM analysis

Under TEM, GO appeared as thin, randomly aggregated stacked sheets with varied edges and highly variable size, ranging from 50 nm to more than 1 μm (Fig. 1A). The GNP was observed as spherical aggregates, with diameters ranging from 20 to 80 nm (Fig. 1B).

Analysis of the control calli revealed cells characterized by large vacuoles containing rare, dispersed material. Their cytoplasm was rich in mitochondria, endoplasmic reticulum, and plastids containing 3-5 starch grains. Furthermore, the large nuclei displayed highly dispersed chromatin (Fig. 1C). In the GO-treated calli, alongside cells exhibiting an ultrastructure similar to the control group, cells with completely disrupted cytoplasm were also observed (Fig. 1D). Some cells contained GO sheets within their vacuoles (Fig. 1E), and occasionally these sheets were even present in the cytoplasm (Fig. 1F).

Conversely, in the cells of GO + Cu-treated calli, pleomorphic nuclei with a large nucleolus were detected. The cytoplasm was characterized by mitochondria lacking evident cristae, unusual plastids with one or two starch grains, and electrondense bodies (Fig. 2A-C). Numerous small vacuoles, occasionally containing one or two small, round and electrondense bodies were also observed (Fig. 2B-C). Within the large central vacuole, structures resembling GO sheets were discernible (Fig. 2D-E).

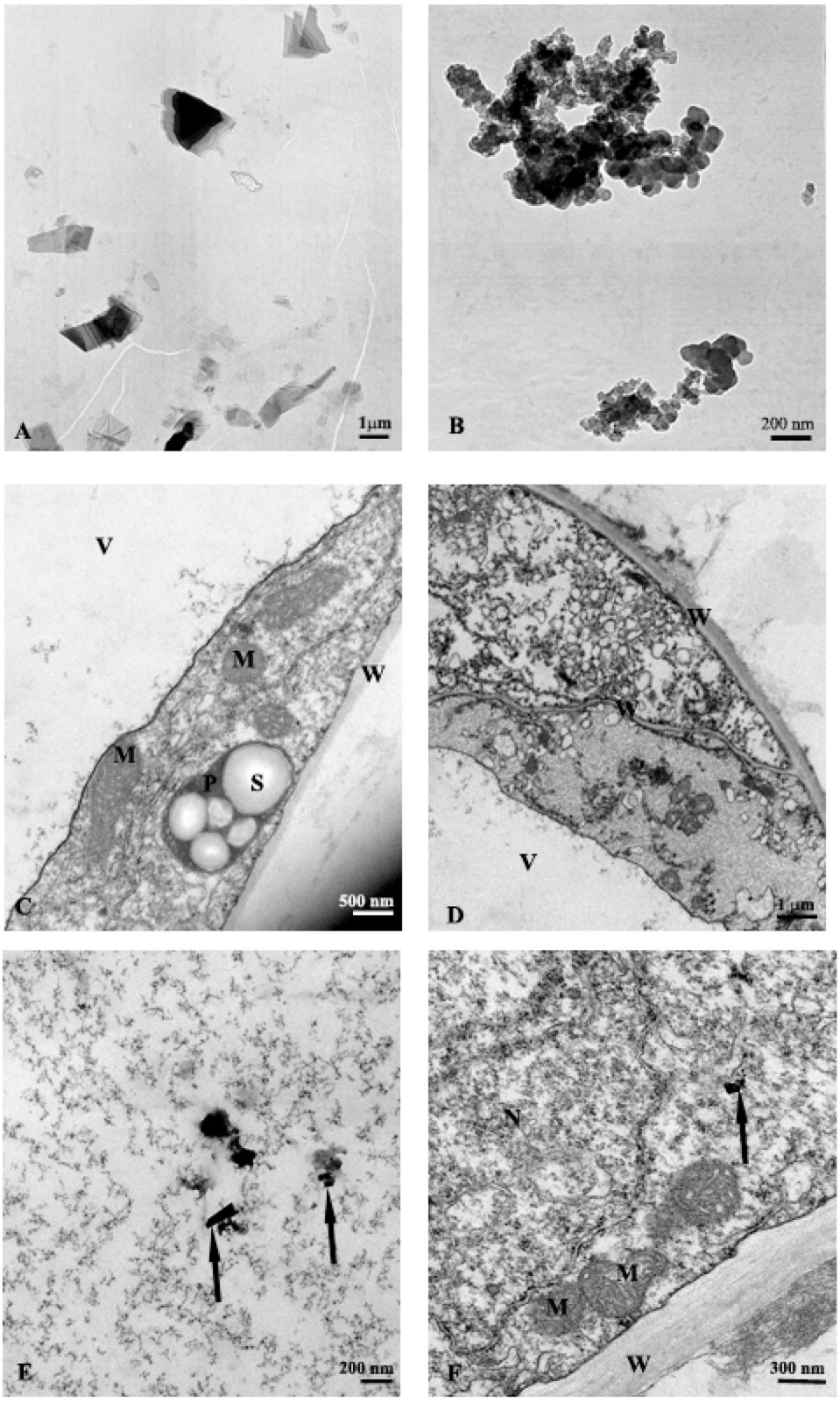

Fig. 1 TEM images of clone 58–861: **A** GO sheets, **B** aggregates of GNP; **C** portions of control culture cells; **D-F** portions of GO-treated culture cells. M, mitochondrion; N, nucleus; P, plastid; S, starch grain; V, vacuole; W, cell wall. The arrows indicate GO sheets

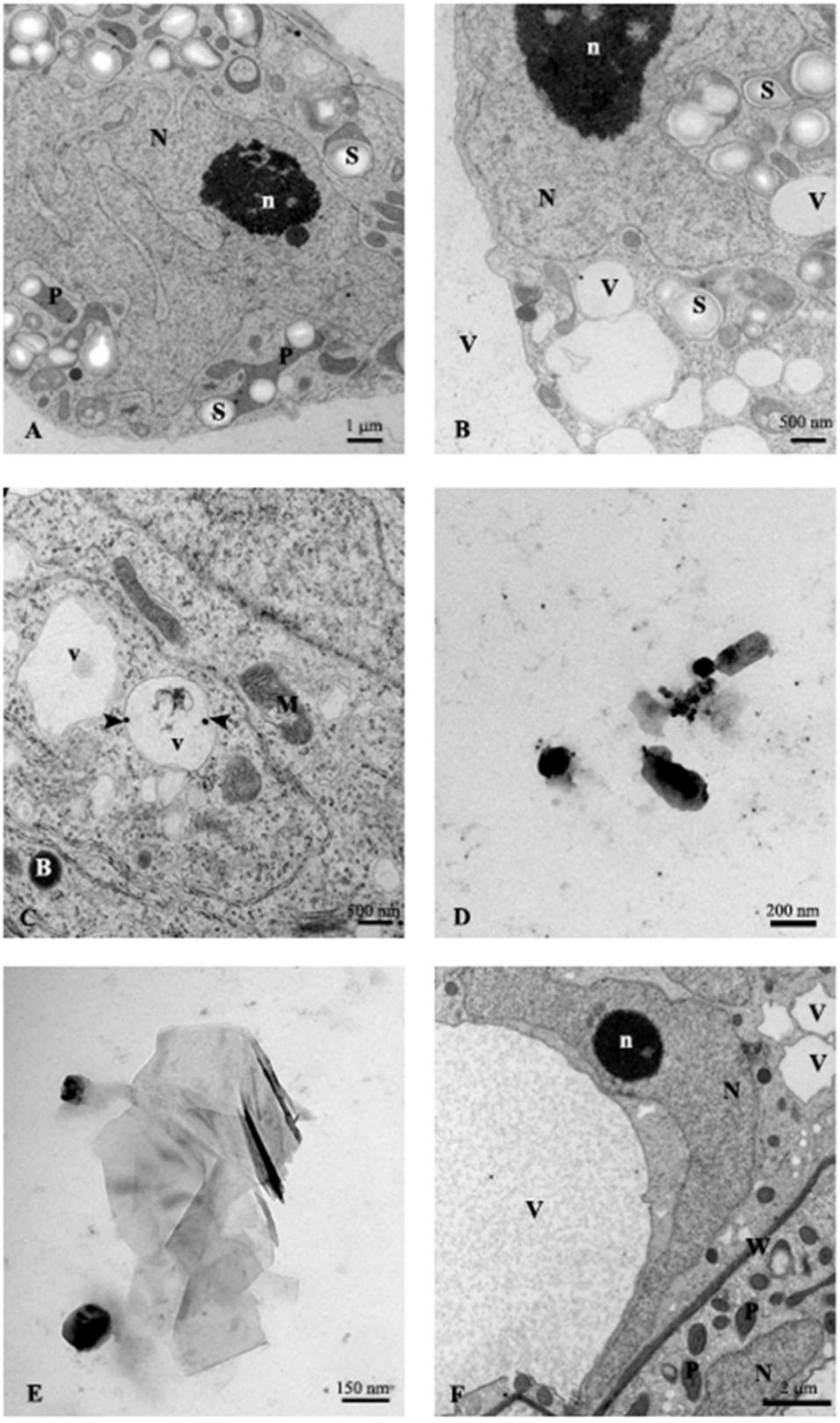

Fig. 2 TEM images of clone 58–861: (**A-E**) portions of GO + Cu-treated culture cells. The arrowheads indicate the electrondense bodies in the vacuoles. (**F**) Portions of GNP-treated culture cells. M, mitochondrion; N, nucleus; n, nucleolus; P, plastid; S, starch grain; V, vacuole; W, cell wall

Following GNP treatment, poplar cells were characterized by large vacuoles abundant in dispersed material (Fig. 2F). Their pleomorphic nuclei contained more condensed chromatin compared to the other treatments and 1-2 nucleoli (Fig. 2A). The cytoplasm featured mitochondria with an electrondense matrix, numerous unusually shaped plastids devoid of starch grains, and electrondense bodies (Fig. 3A-B). The endoplasmic reticulum frequently appeared to expand, forming vesicles and small, seemingly empty vacuoles (Fig. 3B). Notably, GNP was not detected in any of the sections examined.

The cells of the GNP + Cu-treated calli were frequently plasmolyzed (Fig. 3C). Their cytoplasm, of unusual appearance, contained organelles that were often unidentifiable, with the exception of large plastids rich in starch granules (Fig. 3C-D). The pleomorphic nuclei displayed an unusual ultrastructure and large nucleoli (Fig. 3D). Vesicles and small vacuoles, often enclosing one or two small electrondense bodies, were evident in the cytoplasm (Fig. 3E). Rarely, small aggregates of GNPs were detected within the vacuoles (Fig. 3F).

Oxidative stress

As shown in Fig. 4A, significant differences in MDA content were detected among treated-callus cultures. After three weeks, a marked increase in MDA levels was observed in poplar calli exposed to either GO or GNP alone compared to the control, with the effect being more pronounced in the GO treatment. The co-presence of GO and Cu in the medium caused a 57% reduction in MDA content compared to GO alone, although the level was still higher (approximately 27%) than control. The GNP + Cu treatment significantly reduced MDA levels, with a 50% decrease compared to the control and 71% compared to GNP alone. In contrast, Cu alone caused only an 18% reduction relative to the control.

As reported in Fig. 4B, when exposed to GO alone, poplar callus cultures showed an approximately 85% enhancement in CAT activity whereas in the presence of GNP, no statistical difference was observed compared to the control. Exposure to GO + Cu significantly affected CAT activity, resulting lower than either the control or GO alone (by 67.5% and 83.5%, respectively). The GNP + Cu treatment led to a 24% reduction in CAT activity with respect to GNP alone, although no statistically significant differences were present relative to the control. Finally, exposure to Cu alone caused a 44% reduction in CAT activity compared to the control.

As shown in Fig. 4C, neither GO nor GNP alone significantly affected APX activity in poplar cells compared to the control. While Cu alone reduced enzymatic activity by 27% in clone 58–861, the most substantial effects were observed when copper was combined with GO or GNP. The GO + Cu and GNP + Cu treatments reduced APX activity by approximately 61% and 49%, respectively, compared to GO and GNP alone.

In clone 58–861, exposure to either GO or GNP alone did not significantly affect GST activity relative to the control (Fig. 4D). The presence of Cu, either alone or in combination with GO or GNP, led to an increase in enzyme activity, although no statistically significant compared to the control.

In this study, callus cultures exposed to GO alone showed a five-fold increase in total protein content compared to the control, while an almost two-fold enhancement was observed in GNP-treated poplar cells (Fig. 5). In calli grown on medium supplemented with GO + Cu, total protein levels were reduced by 63% relative to GO alone, still resulting in a higher protein content compared to the control. When exposed to GNP + Cu, clone 58–861 showed a 65% decrease in protein accumulation compared to GNP alone, although not statistically different from the control. Notably, the presence of Cu alone in the medium had no effect on total protein content.

H^+-ATPase activity

In poplar cells, as reported in Fig. 6A, exposure to GO alone had no effect on plasma membrane H^+-ATPase levels. Conversely, the co-presence of GO and Cu led to a notable increase in enzyme abundance, compared to both the control and Cu-treated cells. Furthermore, GNP alone caused a slight increase in H^+-ATPase relative to the control and GO-treated cells. However, the combined exposure of GNP and Cu resulted in a reduction of the proton pump's levels.

Interestingly, H^+-ATPase activity is not correlated with plasma membrane enzyme levels. As shown in Fig. 6B, across all treatments, a significant reduction in H^+-ATPase activity was observed in clone 58–861 when compared to the control. Both GO and GNP alone reduced H^+-ATPase activity. The addition of Cu, either alone or in combination with GO or GNP, led to a further decrease, in the order GO + Cu > Cu > GNP + Cu.

Cu and nutrient uptake

As summarized in Table 3, a significant difference in Cu uptake was observed in the treated cells. Specifically, in clone 58–861, the Cu content increased in the following order: Cu > GO + Cu > GNP + Cu. The adsorption kinetic assay performed in demineralized water demonstrated a differential behaviour between GO and GNP regarding their potential role as Cu carriers into the callus cells. Generally, adsorption was rapid, with equilibrium reached within one hour (Supplementary Fig. S1). Specifically, GO exhibited higher adsorption efficiency, binding up to 40% of the Cu (despite the non-optimal pH for adsorption), whereas GNP adsorption levelled off at less than 15%.

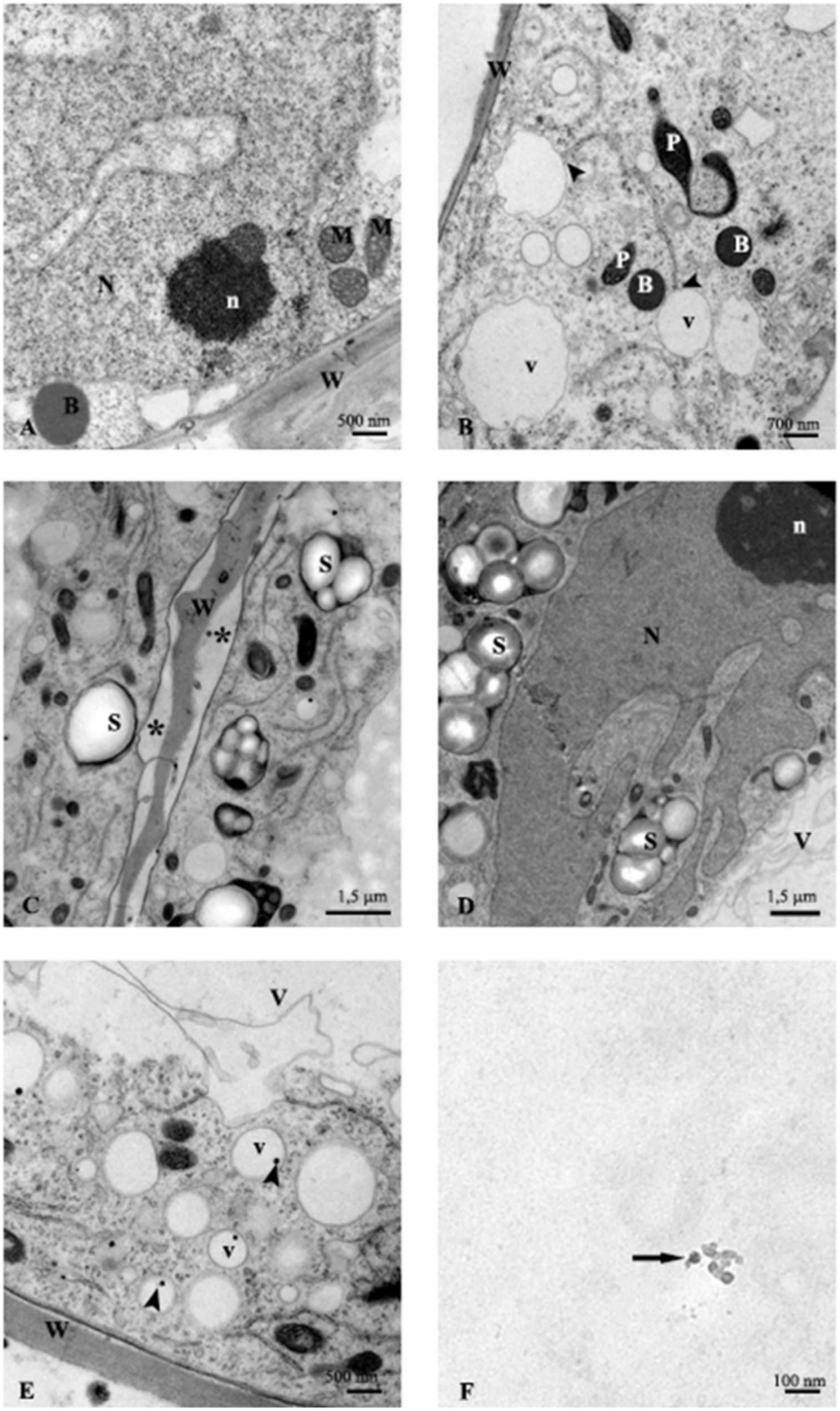
A
N
n
M
M
W
B
500 nm
B
W
P
P
B
B
v
v
700 nm
C
S
W
*
S
*
1,5 µm
D
n
N
S
S
V
1,5 µm
E
V
v
v
W
500 nm
F
100 nm

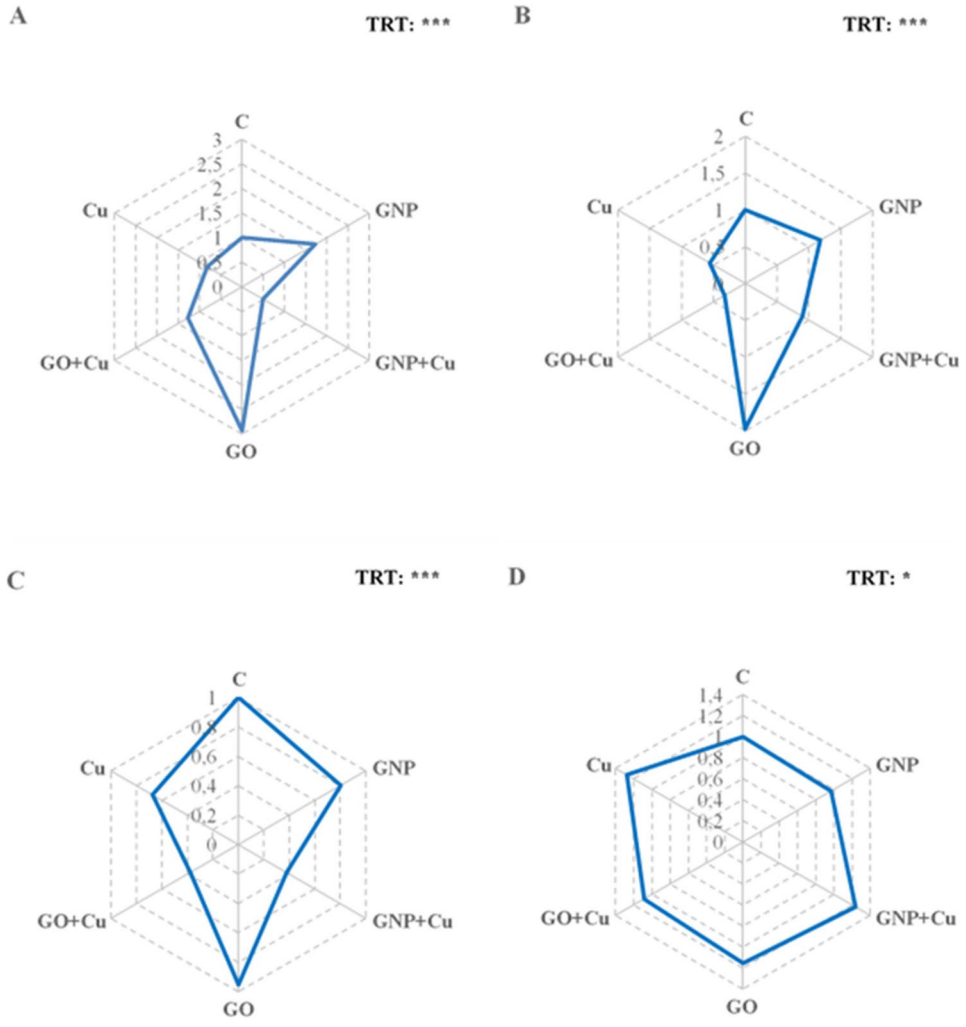

Fig. 4 Radar plot representation of lipid peroxidation content (MDA) (**A**), catalase (**B**), ascorbate peroxidase (**C**) and glutathione S-transferase (**D**) activities in callus cultures of *P. nigra* clone 58–861 exposed for 3 weeks to Cu alone, GO and GNP with or without Cu. Data represent the mean of three biological replicates, with values normalized to the control condition (0 mg/L = control = 1). A detailed Tukey's test ($p < 0.05$) was performed prior to normalization and the results are available in Supplementary Table S1

In poplar cell cultures, micro- and macronutrient uptake differed significantly across the various treatments. In detail, GO exposure led to a marked increase in the levels of all measured elements. When GO and Cu were combined, the concentrations of most macro- and micronutrients decreased to levels similar to control and Cu-treated cells, although calcium (Ca), magnesium (Mg), and sodium (Na) concentrations remained slightly higher than the control.

GNP treatment increased the concentrations of boron (B), Ca, Mg, sulfur (S) and Na relative to the control. However, this effect was notably less marked than the impact of GO. The presence of GNP + Cu in the growth medium led to a reduction in the uptake of B, Mg, S and Na. Other element levels were unaffected, except Ca, which showed a higher concentration than the control.

Principal component analysis (PCA)

The first two components of the PCA explained 75.7% of the total variance in the dataset (Dim1: 49.5%; Dim2: 26.2%) (Fig. 7A), summarizing the complex physiological and biochemical responses of clone 58–861 to the different treatments. Dim1 was positively correlated with CAT ($r = 0.94$), APX ($r = 0.84$), and to a lesser extent GST ($r = 0.61$) enzymatic activities, as well as with water ($r = 0.74$), Ca ($r = 0.73$), and protein ($r = 0.74$) contents. It was negatively correlated with DW (r = -0.92) and Cu content (r = -0.82). Along Dimension 1, a clear distinction emerged between Cu-exposed and Cu-free treatments.

Dim2 was positively correlated with Ca ($r = 0.61$) and protein content ($r = 0.66$), while being negatively correlated with ATPase activity (r = -0.82). A weaker negative correlation was also present with GST (r = -0.69) and MDA (r = -0.57). On Dimension 2, we observed a

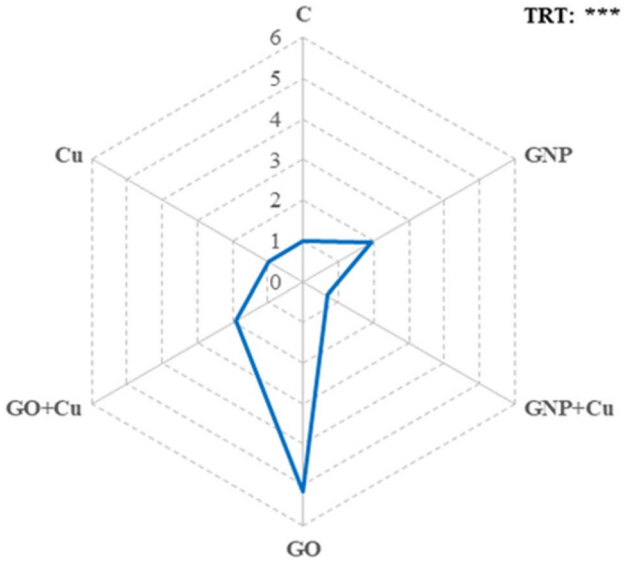

Fig. 5 Radar plot representation of total protein content in callus cultures of *P. nigra* clone 58–861 exposed for 3 weeks to Cu alone, GO and GNP with or without Cu. Data represent the mean of three biological replicates, with values normalized to the control condition (0 mg/L = control = 1). A detailed Tukey's test ($p < 0.05$) was performed prior to normalization and the results are available in Supplementary Table S1

clear separation between GO-treated samples (GO and GO + Cu) and the other samples (C, GNP, and GNP + Cu). Overall, the two dimensions of the PCA clearly distinguished samples based on their treatment, revealing six distinct, non-overlapping clusters with 95% confidence interval ellipses (Fig. 7B). The GO treatment clustered within the positive quadrants of both Dim1 and Dim2, primarily associated with protein synthesis and Ca content, showing a clear divergence from Cu and GNP + Cu treatments, which localized in the negative regions of both axes. The GO + Cu treatment was located in the negative Dim1 and positive Dim2 quadrant, associated with FW and Cu content, contrasting with C and GNP treatment, closely positioned in the positive Dim1 and negative Dim2 quadrant.

Discussion

In this work, to investigate the combined effects of GO + Cu and GNP + Cu on callus cultures of *P. nigra* clone 58–861, we selected the Cu concentration that caused a 20% reduction (EC_{20}) in fresh weight. Employing sub-lethal concentrations enables the investigation of long-term and chronic effects on plant health that might be masked by acute toxicity tests. This approach is highly relevant to natural environments, where heavy metals often occur at low but persistent levels posing a risk of bioaccumulation and complex interactions with other contaminants. This underscores the importance of such studies [40].

Interactions among environmental stressors within plants can occur through various mechanisms, affecting both the magnitude and characteristics of their individual impacts. To evaluate phytotoxicity, plant growth is frequently employed as a crucial physiological parameter. Most studies on the interaction between graphene-based materials and higher plants have reported both

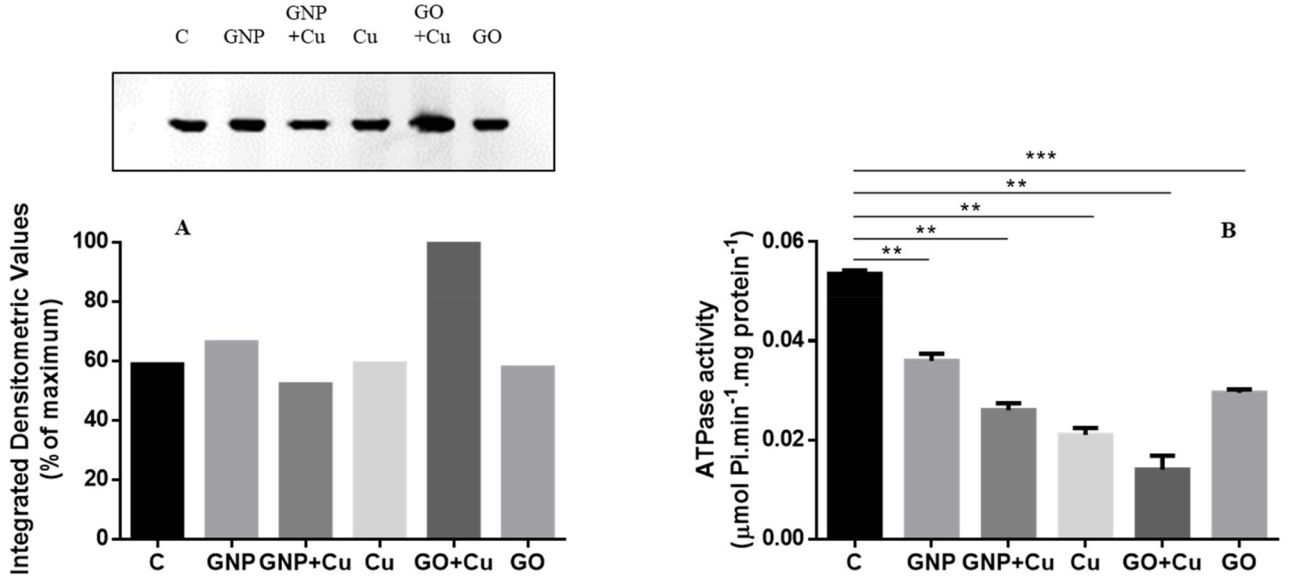

Fig. 6 Plasma membrane H^+-ATPase levels and activity of poplar callus cultures exposed for 3 weeks to Cu alone, GO and GNP with or without Cu. (**A**) Western blot analysis of plasma membrane proteins. Twenty µg of plasma membrane purified fractions were separated by SDS-PAGE, blotted onto PVDF membrane, and immunodecorated with polyclonal anti-H^+-ATPase antibodies. The full-length blot is included in "Supplementary File". (**B**) Vanadate-sensitive phosphohydrolytic activity of H^+-ATPase from plasma membrane fractions. Data represent the mean of three biological replicates. Statistical significance was assessed by Tukey's test, and asterisks indicate statistical differences respect to the Control (**, $p < 0.01$; ***, $p < 0.001$)

Table 3 Effects of GO, GNP and Cu, either alone or in combination, on Cu and nutrient uptake in clone 58–861

	B (mg/g DW)	Ca (mg/g DW)	Cu (mg/g DW) *	Fe (mg/g DW)	K (mg/g DW)	Mg (mg/g DW)	P (mg/g DW)	Mo (mg/g DW)	S (mg/g DW)	Na (mg/g DW)
Control	0.433 ± 0.01^{c}	14.3 ± 0.6^{d}	0.020 ± 0.003^{c}	3.86 ± 1.54^{b}	23.11 ± 7.3^{b}	2.48 ± 0.3^{c}	47.85 ± 17.65^{bc}	0.064 ± 0.037^{ab}	41.08 ± 6.35^{c}	2.86 ± 0.81^{c}
GNP	1.129 ± 0.22^{b}	19.5 ± 0.97^{b}	0.026 ± 0.002^{c}	4.84 ± 0.58^{ab}	27.18 ± 6.28^{b}	3.56 ± 0.10^{b}	63.43 ± 14.67^{b}	0.058 ± 0.009^{ab}	56.61 ± 7.81^{b}	7.44 ± 0.23^{b}
GNP + Cu	0.137 ± 0.04^{d}	16.15 ± 0.50^{c}	2.093 ± 0.3^{b}	3.28 ± 0.68^{b}	13.14 ± 1.08^{c}	2.48 ± 0.11^{c}	28.29 ± 2.85^{c}	0.040 ± 0.013^{b}	29.39 ± 2.68^{d}	0.61 ± 0.08^{d}
GO	3.635 ± 0.14^{a}	74.52 ± 3.84^{a}	0.026 ± 0.002^{c}	10.62 ± 1.20^{a}	55.02 ± 7.17^{a}	11.8 ± 0.63^{a}	141.1 ± 4.26^{a}	0.131 ± 0.036^{a}	150.02 ± 11.84^{a}	33.34 ± 3.37^{a}
GO + Cu	0.622 ± 0.04^{c}	20.87 ± 0.42^{b}	2.48 ± 0.39^{ab}	3.56 ± 0.38^{b}	28.47 ± 0.86^{b}	3.26 ± 0.08^{b}	49.8 ± 7.92^{b}	0.036 ± 0.004^{b}	46.42 ± 3.31^{bc}	5.28 ± 0.90^{b}
Cu	0.470 ± 0.03^{c}	16 ± 1.29^{cd}	3.34 ± 0.48^{a}	5.99 ± 0.52^{ab}	20.77 ± 1.89^{b}	2.54 ± 0.31^{c}	51.01 ± 4.86^{b}	0.084 ± 0.01^{ab}	44.46 ± 1.38^{bc}	5.7 ± 1.42^{b}

Data represent the mean ± SD ($n = 3$)

Different letters indicate statistically significant differences ($p \leq 0.05$, Tukey's test)

* Cu > GO + Cu > GNP + Cu

stimulatory and inhibitory effects on plant growth and development, depending on plant species, the specific experimental conditions and concentration, exposure time, and physicochemical properties of nanostructures [1, 14]. The presence of GO alone significantly reduced the dry weight of poplar cells compared to the control, while increasing their water content. Analogously, treatment with GNP led to a decrease in cellular dry weight, though to a lesser extent than with GO, accompanied by an increase in water content. Notably, structural analysis confirmed the absence of plasmolysis, a finding that contrasts with observations in *Chlorella vulgaris* [41] and *Brassica napus* L [42] treated with GO. Although the exact mechanism by which nanomaterials, like GO, affect plant growth remains unclear, it is plausible that this effect is associated with the upregulation of aquaporin genes, which are essential for maintaining proper plant-water relations. This hypothesis is supported by Khodakovskaya et al. [43] who observed aquaporin activation in tobacco cells treated with carbon nanotubes.

The combined presence of GO and Cu in the growth medium led to a notable increase in poplar cell dry weight, while their water content remained comparable to that of the control. Similarly, the co-presence of GNP and Cu led to a marked enhancement in the dry weight of poplar cells compared to the control. This effect, however, was accompanied by a notable reduction in water content, as confirmed by TEM, which revealed frequent plasmolysis in GNP + Cu-treated callus cells. It is plausible that the observed increase in dry weight stems from the presence of starch granules within plastids. This aligns with findings by Hu et al. [44], who suggested that starch accumulation may be linked to cellular stress adaptation mechanisms.

Moreover, it is well known that changes in plant growth and development are associated with the uptake of macro- and micronutrients, which are essential for various physiological and metabolic pathways [45, 46]. Although the phytotoxicity of GO has received extensive attention, few studies have examined its impact on plant nutrient uptake [47, 48]. For instance, in the presence of increasing GO concentrations, a downward trend in the levels of N, K, Fe, Zn, Mo, B and Si was observed in white clover (*Trifolium repens* L.) [49] while a reduction in the contents of macro- (K, P, N, Mg) and micronutrients (Zn, Mo, Fe, B, Si) occurred in alfalfa (*Medicago sativa* L.) [50]. Similarly, Zhang et al. [51] found a decrease in the levels of N, K, Ca, Mg, Fe, Zn and Cu in wheat seedlings (*Triticum aestivum* L.) exposed to different concentrations of graphene. In the current work, in the presence of GO, the poplar clone exhibited a marked increase in the levels of all measured nutrients, whereas the GNP treatment enhanced only the concentrations of B, Ca, Mg, S, and Na. These results likely stem from the surface

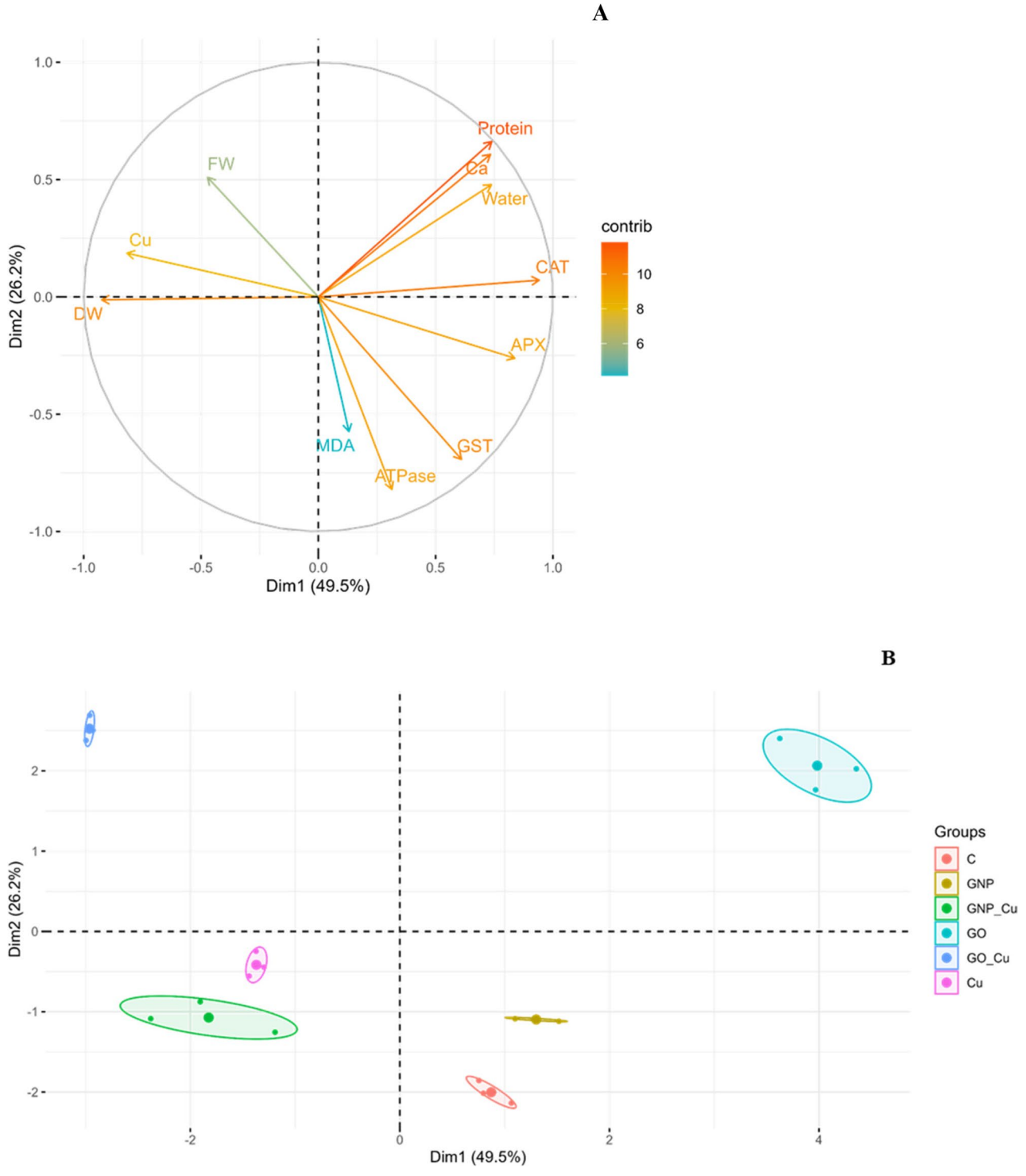

Fig. 7 Principal Component Analysis (PCA) of biological responses of poplar callus cultures exposed to Cu alone, GO and GNP with or without Cu. (**A**) Variables plot illustrating the contributions and correlations of measured parameters to the principal components. Vectors indicate the direction and strength of correlation with the dimensions. Colour intensity (blue to orange/red) reflects the variable's contribution to the displayed components. Variables are: FW, DW, Water content, Protein content, Cu content, Ca content, APX, CAT, MDA, GST, ATPase activity. Both plots are projected onto the first two principal components (Dim1: 49.5% explained variance; Dim2: 26.2% explained variance). (**B**) Individuals plot showing the clustering of samples based on treatment. Each point represents an individual replicate, coloured by treatment group (C, GNP, GNP + Cu, GO, GO + Cu, Cu). Ellipses represent 95% confidence intervals for group centroids

chemistry of the nanomaterials. GO's higher density of oxygen-containing functional groups increases its hydrophilicity compared to GNPs, promoting the rearrangement of lipid membranes and the formation of new pores in the cell wall, thereby enhancing membrane permeability, water uptake, and nutrient transport, as reported in other studies [21, 43, 52]. The co-presence of Cu in the growth medium differentially affected nutrient levels in poplar cells treated with GO and GNP. In detail, following GO + Cu exposure, the concentrations of Ca, Mg, and Na were higher than those in the control. In contrast, in the presence of GNP + Cu treatment, only the Ca level increased with respect to the control. The maintenance of Ca homeostasis within the cell is crucial as it contributes to cell wall and membrane integrity and functions as a second messenger in many physiological processes, including stress response [53].

Regarding intracellular Cu accumulation, the results showed that 25 mg/L of GO promoted metal uptake in poplar cell culture, resulting in a higher content than with either GNP + Cu or Cu alone. Previous studies have reported GO's impact on the metal uptake in plants. For instance, the co-presence of carboxylated graphene oxide-chitosan spheres (GO-COOH/CS) reduced Cu bioaccumulation in wheat seedlings from Cu^{2+} polluted soil [25] while Cu uptake in *Lemna minor* L. was decreased by the addition of GO (5 mg/L) in a 20 μM Cu^{2+} aqueous solution [2]. These findings were attributed to the adsorption of Cu^{2+} onto the GO surface, thereby mitigating metal accumulation and toxicity. Conversely, at high GO concentration, enhanced Cd levels were observed in rice [26] and wheat [3], which is consistent with our results. It is plausible that oxygen functional groups allow GO to efficiently adsorb Cu and act as a carrier, keeping this metal readily available for uptake by poplar cell culture, as reported by Kabiri et al. [4].

Previous investigations have shown that graphene nanomaterials can trigger reactive oxygen species (ROS) generation within plant cells. Increased ROS levels cause oxidative stress, leading to metabolic alterations, dysfunctions and affecting membrane fluidity and permeability. Therefore, maintaining the balance between ROS production and elimination is crucial for redox homeostasis and the physiological activities of plants [54].

The plasma membrane acts as the primary barrier, regulating the transport of substances - including toxic ones - and triggering signalling pathways to mitigate their effects. How graphene nanomaterials interact with the plasma membrane remains to be fully elucidated, as the process varies significantly with concentration, physicochemical properties, and plant species. Recent findings by Li et al. [55] reported a downregulation of proteins related to endocytosis in pepper plants treated with graphene derivatives (GO, rGO, and GOQDs). These results suggest that endocytosis may be involved in plant graphene nanomaterial uptake; however, further investigation is required to fully elucidate the mechanism for the internalization of graphene nanomaterials in plant cells. In this study, TEM observations revealed the presence of GO in both the cytoplasm and the vacuole, thereby confirming its internalization into the cell following treatment with GO alone and in co-presence with Cu. Likewise, small aggregates identifiable as GNP were detected in the vacuole, though only in cells treated with GNP + Cu. These outcomes are consistent with those of Marcote et al. [56], who observed that endocytosed markers in plant cells ultimately accumulate in the vacuoles. It's plausible that the vacuolar confinement of these materials, along with the increased number of starch granules observed by TEM, represents a cellular self-defence strategy to limit their impact on cellular physiological activity, as previously reported [42, 44]. The internalization induced ultrastructural alterations of varying intensity, specifically targeting mitochondria and plastids, as evidenced by TEM, thereby contributing to oxidative stress. The extent of such oxidative damage can be indicated by malondialdehyde (MDA), which is the major product of membrane lipid peroxidation [1, 29]. Our findings showed that after 21 days, both GO and GNP treatments induced a significant increase in MDA levels compared with the control, exhibiting a more pronounced effect with GO. These findings align with those of Anjum et al. [57], who reported increased MDA levels in *Vicia Faba* L. exposed to increasing GO concentrations. Similarly, a rise in MDA content was detected in *Aloe vera* L. at high GO concentrations [58]. Notwithstanding the results, lipid peroxidation did not emerge as a primary factor differentiating the treatments under the experimental conditions, as shown by PCA.

The co-presence of GNP and Cu resulted in a significant decrease in MDA content relative to the control, GNP alone, or Cu alone. Conversely, under GO + Cu treatment, MDA levels were reduced by 56.7% compared with GO alone, remaining still higher than in the control and Cu-treated cells. To the best of the authors' knowledge, research on the mutual effects of GO and metals is scarce, with a notable lack of analysis regarding their combined impact on the oxidative stress response. According to Muszyńska and Labudda [23], some heavy metals, such as Cu, exhibit a dual role and at low concentrations, contribute to the mitigation of oxidative stress in plants under stress conditions. Their involvement includes, but is not limited to, the maintenance of redox and ionic balance. For example, Wu et al. [59] found that Mo supplementation reduced the level of lipid peroxidation marker in *T. aestivum* under drought stress.

To counteract the high levels of ROS and oxidative stress, plants activate a well-regulated antioxidant

machinery involving several enzymatic and non-enzymatic components that work synergistically to achieve ROS homeostasis [60]. Among the ROS species, H_2O_2 is regarded as a crucial redox molecule, due to its remarkable stability and its capacity to act as a signaling molecule, modulating several downstream reactions, such as cell differentiation, cell wall formation and stress response [61, 62]. In the antioxidant system, catalase (CAT), ascorbate peroxidase (APX) and glutathione S-transferase (GST) enzymes are considered effective scavengers of H_2O_2. Specifically, CAT is crucial for maintaining redox balance during oxidative stress, while APX plays a critical role in controlling intracellular H_2O_2 levels. GST plays multiple roles in stress tolerance, including binding metal ions via glutathione's SH group and reducing the oxidative stress-induced accumulation of H_2O_2 and MDA [60]. In this study, the presence of GO in the growth medium caused a marked enhancement in CAT activity, while no effect was observed on APX and GST activities compared to the control. While the co-presence of Cu had no effect on GST activity, it notably decreased both CAT and APX activities compared to GO alone and the control. In contrast, GNP treatment alone did not affect the activity of any of these enzymes compared with the control.

GO and GNP have been shown to affect plant physiological responses by either modulating antioxidant defences at low concentrations or inducing severe oxidative stress at higher doses [14]. In our study the interaction between GNP and Cu resulted in a pronounced decrease in APX activity when compared to both the control and GNP alone. The inhibition of enzymatic activities could be associated with the decrease in soluble protein content. Our findings showed that, in clone 58–861, the presence of GO alone led to a marked increase in protein content compared with the control. Our results align with Zhao et al. [50], who reported an increase in protein levels in alfalfa (*M. sativa* L.) exposed to a low GO concentration. The co-presence with Cu significantly reduced the protein content, yet it remained higher than control. Following GNP treatment, an enhancement in protein levels was observed. Conversely, the co-presence of Cu induced a reduction compared to GNP alone, yet not statistically different from levels observed in control and Cu alone. The scarcity of information in the existing literature on the interactions among Cu, GO or GNP, and antioxidant enzymes makes it difficult to draw comparisons with other systems. Regardless, the sharp decline in CAT and APX activities, accompanied by a significant reduction in total protein content, suggests that these enzymes are primary targets of Cu-induced toxicity. This effect is particularly evident in the GO + Cu treatment, indicating enzymatic inhibition or impaired protein synthesis - potentially triggered by the direct binding of Cu ions to functional sulfhydryl groups or the displacement of essential metal cofactors - rather than a diminished requirement for ROS scavenging [63–65]. TEM observations corroborated these findings, revealing that Cu addition - specifically to GNP-triggered mitochondrial alterations and affected nuclear morphology, characterized by significant chromatin condensation.

Recently, several studies have investigated the link between plasma membrane (PM) H^+-ATPase and ROS signalling in plant response to abiotic stress [53, 62]. Membrane damage, caused by oxidative stress, induces ionic disturbances in cells. Under such conditions, the plasma membrane (PM) H^+-ATPase plays a key role in regulating ion homeostasis by enhancing membrane potential generation and supplying the proton motive force for secondary active transport [66]. It is worth noting that no previous work has investigated the effect of GO and GNP on this proton pump's activity. In the current study, in clone 58–861, H^+-ATPase levels remained unaffected by GO treatment even though they exhibited a slight increment in the presence of GNP. Notably, both conditions were associated with a reduction in ATPase activity relative to the control. About GNP, the addition of Cu in the growth medium led to a reduction both in H^+-ATPase levels and activity compared to GNP alone and control. Conversely, the co-treatment of GO and Cu led to a significant reduction in ATPase activity despite increased enzyme levels at the membrane. The strong inhibitory effect on H^+-ATPase activity observed across all treatments did not correlate with the enzyme's membrane levels. This discrepancy suggests a direct effect of GNP and GO on proton pump activity, likely mediated by post-translational mechanisms, including the well-known regulatory event involving the phosphorylation of a threonine residue at the extreme C terminus of the enzyme and the subsequent binding of 14-3-3 proteins. Additionally, since it is well known that Cu is a H^+-ATPase inhibitor, inducing half-maximal inhibition at 2–5 μM [67], the strong inhibitory effect of GNP + Cu and GO + Cu can be attributed to the combination of copper's toxic effects and the enzyme's post-translational regulation. Since the H^+-ATPase provides the primary motive force for secondary active transport, the inhibition of the proton pump observed upon co-exposure to GO + Cu and GNP + Cu is apparently at odds with the general increase in nutrient levels detected in this study. This apparent paradox can be reconciled by considering a shift from active to passive transport mechanisms. The nanomaterials may directly affect membrane permeability, a hypothesis supported by the observed increase in water uptake. These results suggest that the elevated nutrient concentrations in the poplar callus are a consequence of increased membrane permeability and passive influx, rather than a stimulation of H^+-ATPase-driven active transport.

The observed results suggest that GO + Cu and GNP + Cu treatments trigger cellular metabolic quiescence. By altering mitochondrial cristae and inhibiting H^+-ATPase, these treatments impair energy production, prompting the cell to shift carbon flow into starch storage rather than antioxidant maintenance. This metabolic shutdown concurrently appears to suppress ROS generation below the threshold required for lipid peroxidation, despite the cell's diminished scavenging capacity. Further studies are required to elucidate the mechanisms underlying this response.

Conclusion

To the best of our knowledge, this study represents the first investigation into the combined effects of Cu and carbon nanomaterials (GO or GNP) on the woody species *Populus nigra* L. (clone 58–861), under in vitro growth conditions. Our results showed that co-occurrence of Cu, at its EC_{20} concentration, and graphene nanomaterials induce a distinct stress phenotype in *P. nigra* callus. This state is characterized by a counterintuitive increase in dry weight and a significant reduction in lipid peroxidation compared to GO or GNP treatments alone; however, this apparent physical recovery is undermined by a severe impairment of the antioxidant defence system.

The interaction between GO and Cu promoted significantly higher intracellular metal uptake than the GNP + Cu treatment, as GO's oxygen-containing functional groups (epoxy, hydroxyl, and carboxyl) facilitate metal complexation more effectively than the inert GNP surface. This suggests that risk assessment for graphene nanomaterials cannot be based on their individual toxicity alone; rather, it must consider their role as potential vectors for co-existing pollutants.

These findings offer new perspectives into the mutual effects of Cu and carbon nanomaterials, providing essential data for the safer environmental application of these materials. Given the available genetic map of *P. nigra*, further research is necessary to better understand the Cu-GO or Cu-GNP-plant interaction at the molecular level.

Although this study utilized in vitro callus cultures, the results provide valuable insights for future in vivo whole plants studies and field experiments, necessary to validate these mechanisms in natural systems.

Supplementary Information

The online version contains supplementary material available at https://doi.org/10.1186/s12870-026-08689-2.

Supplementary Material 1.

Acknowledgements
Not applicable.

Authors' contributions
S.M.: Writing – review & editing, Writing – original draft, Methodology, Formal analysis; M.A.I.: Writing – review & editing, Methodology, Formal analysis; B.C.: Writing – review & editing, Methodology, Formal analysis, Resources; L.C.: Writing – review & editing, Methodology, Formal analysis; A.F.: Writing – review & editing, Methodology, Formal analysis; D.G.: Writing – review & editing, Data curation; M.M.: Writing - review & editing, Methodology; V.G.M.: Writing – review & editing, Methodology, Formal analysis, Data curation; V.I.: Writing – original draft, Writing – review & editing, Methodology, Visualization, Resources, Formal analysis, Supervision, Investigation, Conceptualization, Data curation.

Funding
This research did not receive any specific grant from funding agencies in the public, commercial, or not-for-profit sectors.

Data availability
The datasets used and/or analysed during the current study are available from the corresponding author on reasonable request.

Declarations

Ethics approval and consent to participate
Not applicable.

Consent for publication
All authors read and approved the final manuscript.

Competing interests
The authors declare no competing interests.

Received: 19 December 2025 / Accepted: 30 March 2026
Published online: 02 April 2026

References

1. Zhang X, Cao H, Wang H, Zhao J, Gao K, Qiao J, Li J, Ge S. The effects of graphene-family nanomaterials on plant growth: a review. Nanomaterials. 2022;12:936.
2. Hu C, Liu L, Li X, Xu Y, Ge Z, Zhao Y. Effect of graphene oxide on copper stress in *Lemna minor* L.: evaluating growth, biochemical responses, and nutrient uptake. J Hazard Mater. 2018;341:168–76.
3. Gao M, Yang Y, Song Z. Toxicity of cadmium to wheat seedling roots in the presence of graphene oxide. Chemosphere. 2019;233:9–16.
4. Kabiri S, Degryse F, Tran DNH, da Silva RC, McLaughlin MJ, Losic D. Graphene Oxide: A New Carrier for Slow Release of Plant Micronutrients. ACS Appl Mater Interfaces. 2017;9:43325–35.
5. Gandhi MR, Vasudevan S, Shibayama A, Yamada M. Graphene and Graphene-Based Composites: A Rising Star in Water Purification - A Comprehensive Overview. Chem Selection. 2016;1:4358–85.
6. Zhao L, Yang ST, Yilihamu A, Wu D. Advances in the applications of graphene adsorbents: from water treatment to soil remediation. Rev Inorg Chem. 2019;39:47–76.
7. Ijaz M, Khan F, Ahmed T, Noman M, Zulfiqar F, Rizwan M, Chen J, Siddique KHM, Li B. Nanobiotechnology to advance stress resilience in plants: Current opportunities and challenges. Mater Today Bio. 2023;22:100759.
8. Khaliha S, Bianchi A, Kovtun A, Tunioli F, Boschi A, Zambianchi M, Melucci M. Graphene oxide nanosheets for drinking water purification by tandem adsorption and microfiltration. Sep Purif Technol. 2022;300:121826.
9. Tunioli F, Khaliha S, Mantovani S, Bianchi A, Kovtun A, Xia Z, Melucci M. Adsorption of emerging contaminants by graphene related materials and their alginate composite hydrogels. J Environ Chem Eng. 2023;11:109566.
10. Sorayani Bafqi MS, Tunioli F, Khaliha S, Melucci M, Saner Okan B. Development of anisotropic nanofibrous hybrid membranes coated with upcycled graphene for enhanced adsorption of emerging contaminants from drinking water. Environ Res. 2025;282:122086.

11. Song J, Cao K, Duan C, Luo N, Cui X. Effects of Graphene on *Larix olgensis* Seedlings and Soil Properties of Haplic Cambisols in Northeast China. Forests. 2020;11:258.
12. Ding X, Pu Y, Tang M, Zhang T. Environmental and health effects of graphene-family nanomaterials: Potential release pathways, transformation, environmental fate and health risks. Nano Today. 2022;42:101379.
13. Hong H, Part F, Nowack B. Prospective Dynamic and Probabilistic Material Flow Analysis of Graphene-Based Materials in Europe from 2004 to 2030. Environ Sci Technol. 2022;56:13798–809.
14. Wang Q, Li C, Wang Y, Que X. Phytotoxicity of Graphene Family Nanomaterials and Its Mechanisms: A Review. Front Chem. 2019;7:292.
15. Guo X, Zhao J, Wang R, Zhang H, Xing B, Naeem M, Yao T, Li R, Xu R, Zhang Z, Wu J. Effects of graphene oxide on tomato growth in different stages. Plant Physiol Biochem. 2021;162:447–55.
16. Zhang X, Cao H, Zhao J, Wang H, Zhang J. Graphene oxide exhibited positive effects on the growth of *Aloe vera* L. *Physiol*. Mol Biol Plants. 2021;27:815–24.
17. Jiao J, Yuan C, Wang J, Xia Z, Xu B. The role of graphene oxide on tobacco root growth and its preliminary mechanism. J Nanosci Nanotechnol. 2016;16:12449–54.
18. Shen S, Liu Y, Wang F, Yao G, Xie L, Xu B. Graphene Oxide Regulates Root Development and Influences IAA Concentration in Rice. J Plant Growth Regul. 2019;38:241–8.
19. Cheng F, Liu YF, Lu GY, Zhang XK, Xie LL, Yuan CF, Xu B. Graphene oxide modulates root growth of Brassica napus L. and regulates ABA and IAA concentration. J Plant Physiol. 2016;193:57–63.
20. Ahmadi SZ, Zahedi B, Ghorbanpour M, Mumivand H. Comparative morpho-physiological and biochemical responses of *Capsicum annuum* L. plants to multi-walled carbon nanotubes, fullerene C60 and graphene nanoplatelets exposure under water deficit stress. BMC Plant Biol. 2024;24:116.
21. Kazlauskas M, Jurgelėnė Ž, Šemčuk S, Jokšas K, Kazlauskienė N, Montvydienė D. Effect of graphene oxide on the uptake, translocation and toxicity of metal mixture to *Lepidium sativum* L. plants: Mitigation of metal phytotoxicity due to nanosorption. Chemosphere. 2023;312:137221.
22. Elumalai P, Gao X, Parthipan P, Luo J, Cui J. Agrochemical pollution: A serious threat to environmental health. Curr Opin Environ Sci Health. 2025;43:100597.
23. Muszyńska E, Labudda M. (2019). Dual role of metallic trace elements in stress biology- from negative to beneficial impact on plants. IJMS. 2019;20:3117.
24. Chen G, Li J, Han H, Du R, Wang X. Physiological and Molecular Mechanisms of Plant Responses to Copper Stress. IJMS. 2022;23:12950.
25. Zhao L, Guan X, Yu B, Ding N, Liu X, Ma Q, Yang S, Yilihamu A, Yang S-T. Carboxylated graphene oxide-chitosan spheres immobilize Cu^{2+} in soil and reduce its bioaccumulation in wheat plants. Environ Int. 2019;133:105208.
26. Li J, Wu F, Fang Q, Wu Z, Duan Q, Li X, Ye W. The mutual effects of graphene oxide nanosheets and cadmium on the growth, cadmium uptake and accumulation in rice. Plant Physiol Biochem. 2020;147:289–94.
27. Rossi L, Sharifan H, Zhang W, Schwab AP, Ma X. Mutual effects and in planta accumulation of co-existing cerium oxide nanoparticles and cadmium in hydroponically grown soybean (*Glycine max* (L.) Merr). Environ Sci: Nano. 2018;5:150–7.
28. Iori V, Pietrini F, Massacci A, Zacchini M. Induction of metal binding compounds and antioxidative defence in callus cultures of two black poplar (*P. nigra*) clones with different tolerance to cadmium. Plant Cell Tiss Organ Cult. 2012;108:17–26.
29. Iori V, Muzzini VG, Venditti I, Casentini B, Iannelli MA. Phytotoxic impact of bifunctionalized silver nanoparticles (AgNPs-Cit-L-Cys) and silver nitrate ($AgNO_3$) on chronically exposed callus cultures of *Populus nigra* L. Environ Sci Pollut Res. 2023;30:116175–85.
30. Confalonieri M, Balestrazzi A, Bisoffi S, Carbonera D. In vitro culture and genetic engineering of Populus spp.: synergy for forest tree improvement. Plant Cell Tissue Organ Cult. 2003;72:109–38.
31. Okan BS, Menceloğlu Y, Ozunlu BG, Yagci YE. Graphene from waste tire by recycling technique for cost-effective and light-weight automotive plastic part production. Cesme-Izmir Turk. 2020;AIP Conf Proc(2205):020046.
32. Murashige T, Skoog F. A Revised Medium for Rapid Growth and Bio Assays with Tobacco Tissue Cultures. Physiol Plant. 1962;15:473–97.
33. Iori V, Giorgetti L, Casentini B, Muzzini VG, Okan BS, Melucci M, Iannelli MA. Graphene effects on *Populus nigra*: assessment of sex-specific adaptive responses by in vitro culture. Plant Cell Tissue Organ Cult. 2025;163:22.
34. Habig WH, Jakoby WB. (1981). Assays for differentiation of glutathione S-Transferases. In: *Methods in Enzymology, Elsevier;* pp. 398–405.
35. Ernst O, Zor T. (2010). Linearization of the Bradford Protein Assay. *JoVE*, 1918.
36. Fiorillo A, Mattei M, Aducci P, Visconti S, Camoni L. The Salt Tolerance Related Protein (STRP) Mediates Cold Stress Responses and Abscisic Acid Signalling in *Arabidopsis thaliana*. Front Plant Sci. 2020;11:1251.
37. Visconti S, D'Ambrosio C, Fiorillo A, Arena S, Muzi C, Zottini M, Camoni L. Overexpression of 14-3-3 proteins enhances cold tolerance and increases levels of stress-responsive proteins of *Arabidopsis* plants. Plant Science. 2019;289:110215.
38. Fiorillo A, Manai M, Visconti S, Camoni L. The Salt Tolerance–Related Protein (STRP) Is a Positive Regulator of the Response to Salt Stress in *Arabidopsis thaliana*. Plants. 2023;12:1704.
39. Fiorillo A, Parmagnani AS, Visconti S, Mannino G, Camoni L, Maffei ME. 14-3-3 Proteins and the Plasma Membrane H^+-ATPase Are Involved in Maize (*Zea mays*) Magnetic Induction. Plants. 2023;12:2887.
40. Li X, Gu AZ, Zhang Y, Xie B, Li D, Chen J. Sub-lethal concentrations of heavy metals induce antibiotic resistance via mutagenesis. J Hazard Mater. 2019;369:9–16.
41. Hu X, Ouyang S, Mu L, An J, Zhou Q. Effects of Graphene Oxide and Oxidized Carbon Nanotubes on the Cellular Division, Microstructure, Uptake, Oxidative Stress, and Metabolic Profiles. Environ Sci Technol. 2015;49:10825–33.
42. Xiao X, Wang X, Liu L, Chen C, Sha A, Li J. Effects of three graphene-based materials on the growth and photosynthesis of *Brassica napus* L. Ecotoxicol Environ Saf. 2022;234:113383.
43. Khodakovskaya MV, De Silva K, Biris AS, Dervishi E, Villagarcia H. Carbon Nanotubes Induce Growth Enhancement of Tobacco Cells. ACS Nano. 2012;6:2128–35.
44. Hu X, Lu K, Mu L, Kang J, Zhou Q. Interactions between graphene oxide and plant cells: regulation of cell morphology, uptake, organelle damage, oxidative effects and metabolic disorders. Carbon. 2014;80:665–76.
45. Fan X, Zhou X, Chen H, Tang M, Xie X. Cross-Talks Between Macro- and Micronutrient Uptake and Signaling in Plants. Front Plant Sci. 2021;12:663477.
46. Ahmed N, Zhang B, Chachar Z, Li J, Xiao G, Wang Q, Tu P. Micronutrients and their effects on Horticultural crop quality, productivity and sustainability. Scientia Horticulturae. 2024;323:112512.
47. Zhu YX, Weng YN, Zhang SY, Liu LJ, Du ST. The nitrate uptake and growth of wheat were more inhibited under single-layer graphene oxide stress compared to multi-layer graphene oxide. Ecotoxicol Environ Saf. 2022;247:114229.
48. Li P, Xia Y, Song K, Liu D. The Impact of Nanomaterials on Photosynthesis and Antioxidant Mechanisms in Gramineae Plants: Research Progress and Future Prospects. Plants. 2024;13:984.
49. Zhao S, Zhu X, Mou M, Wang Z, Duo L. Assessment of graphene oxide toxicity on the growth and nutrient levels of white clover (*Trifolium repens* L). Ecotoxicol Environ Saf. 2022;234:113399.
50. Zhao S, Wang W, Chen X, Gao Y, Wu X, Ding M, Duo L. Graphene oxide affected root growth, anatomy, and nutrient uptake in alfalfa. Ecotoxicol Environ Saf. 2023;250:114483.
51. Zhang P, Zhang R, Fang X, Song T, Cai X, Liu H, Du S. Toxic effects of graphene on the growth and nutritional levels of wheat (*Triticum aestivum* L.): short- and long-term exposure studies. J Hazard Mater. 2016;317:543–51.
52. He Y, Hu R, Zhong Y, Zhao X, Chen Q, Zhu H. Graphene oxide as a water transporter promoting germination of plants in soil. Nano Res. 2018;11:1928–37.
53. Thor K. Calcium—Nutrient and Messenger. Front Plant Sci. 2019;10:440.
54. Zhou S, Wang W, Wang P, Ma H, Li W. The role of reactive oxygen species in regulation of the plasma membrane H^+-ATPase activity in Masson pine (*Pinus massoniana* Lamb.) roots responding to acid stress. Tree Physiol. 2024;44:tpae083.
55. Li X, Sun S, Guo S, Hu X. Identifying the phytotoxicity and defense mechanisms associated with graphene-based nanomaterials by integrating multiomics and regular analysis. Environ Sci Technol. 2021;55:9938–48.
56. Marcote MJ, Gu F, Gruenberg J, Aniento F. Membrane transport in the endocytic pathway: animal versus plant cells. Protoplasma. 2000;210:123–32.
57. Anjum NA, Singh N, Singh MK, Sayeed I, Duarte AC, Pereira E, Ahmad I. Single-bilayer graphene oxide sheet impacts and underlying potential mechanism assessment in germinating faba bean (*Vicia faba* L). Sci Total Environ. 2014;472:834–41.
58. Zhang X, Cao H, Zhao J, Wang H, Xing B, Chen Z, Li X, Zhang J. Graphene oxide exhibited positive effects on the growth of *Aloe vera* L. Physiol Mol Biol Plants. 2021;27:815–24.
59. Wu S, Hu C, Tan Q, Xu S, Sun X. Nitric Oxide Mediates Molybdenum-Induced Antioxidant Defense in Wheat under Drought Stress. Front Plant Sci. 2017;8:1085.
60. Rajput VD, Harish, Singh RK, Verma KK, Sharma L, Quiroz-Figueroa FR, Mandzhieva S. Recent Developments in Enzymatic Antioxidant Defence

Mechanism in Plants with Special Reference to Abiotic Stress. Biology. 2021;10:267.
61. Kärkönen A, Kuchitsu K. Reactive oxygen species in cell wall metabolism and development in plants. Phytochemistry. 2015;112:22–32.
62. Huang Y, Cao H, Yang L, Chen C, Shabala L, Xiong M, Shabala S. Tissue-specific respiratory burst oxidase homolog-dependent H_2O_2 signaling to the plasma membrane H^+-ATPase confers potassium uptake and salinity tolerance in Cucurbitaceae. J Exp Bot. 2019;70:5879–93.
63. Mazhoudi S, Chaoui A, Habib Ghorbal M, El Ferjani E. Response of antioxidant enzymes to excess copper in tomato (*Lycopersicon esculentum*, Mill). Plant Sci. 1997;127:129–37.
64. Contreras RA, Pizarro M, Köhler H, Sáez CA, Zúniga GE. Copper stress induces antioxidant responses and accumulation of sugars and phytochelatins in Antartic Colobanthus quitensis (Kunth) Bartl. Biol Res. 2018;51(1):48.
65. Ye N, Li H, Zhu G, Liu Y, Liu R, Xu W, Jing Y, Peng X, Zhang J. Copper suppresses abscisic acid catabolism and catalase activity, and inhibits seed germination of rice. Plant Cell Physiol. 2014;55(1):2008–16.
66. Falhof J, Pedersen JT, Fuglsang AT, Palmgren M. Plasma Membrane H^+ -ATPase Regulation in the Center of Plant Physiology. Mol Plant. 2016;9:323–37.
67. Janicka-Russak M, Kabala K, Burzynski M. Different effect of cadmium and copper on H^+-ATPase activity in plasma membrane vesicles from *Cucumis sativus* roots. J Exp Bot. 2012;63:4133–42.

Publisher's Note